

Kenaf Bast Nanocrystalline Cellulose: Analysis of Morphological, Chemical, Crystalline, and Thermal

Rudi Dungani,^{a,*} Lili Melani,^a Widya Fatriasari,^b Sasa Sofyan Munawar,^c Firda Aulya Syamani,^b Melbi Mahardika,^b Tati Karliati,^a Mustika Dewi,^a Alpihan,^d and Wahyu Supriyati^d

Cellulose nanocrystals (CNC) were prepared from delignified kenaf bast fiber by using alkaline pulping, based on soda anthraquinone, hydrogen peroxide bleaching, and acid hydrolysis treatment with H₂SO₄. The size and morphology of the fibers were characterized by scanning electron microscopy (SEM), and the isolated fiber from unbleached and bleached pulp had a diameter between 9 to 30 μm. Fourier transform infrared (FTIR) spectroscopy exhibited that the content of lignin decreased in the pulping process, and the lignin was almost completely removed during hydrogen peroxide bleaching. Moreover, fibers were characterized for crystallinity using X-ray diffraction (XRD). The fiber crystallinity gradually increased at each stage of the process (raw kenaf bast, unbleached pulp, bleached pulp, and acid hydrolysis). The fiber was characterized by atomic force microscopy (AFM), which showed that the isolated pulp nanofibers had diameters of approximately 30 nm.

DOI: 10.15376/biores.18.4.6913-6928

Keywords: Alkaline; Kenaf; Nanofibers; Pulping; SEM

Contact information: a: School Life Sciences and Technology, Institut Teknologi Bandung, Bandung 40132, Indonesia; b: Research Center for Biomass and Bioproducts, National Research and Innovation Agency, Bogor 16610, Indonesia; c: Research Center for Environmental and Clear Technology, National Research and Innovation Agency, Bandung 40135, Indonesia; d: Department of Forestry, Faculty of Agricultural, Palangka Raya University, Palangka Raya 74874, Center Kalimantan, Indonesia; *Corresponding author: dunganir@gmail.com

INTRODUCTION

Cellulose and nano-size cellulose particles have generated industrial and scientific interest as novel biomaterials. Cellulose is environmentally friendly and renewable, and it is a multi-serviceable raw material that can substitute for numerous materials that are not renewable (Achukwu *et al.* 2022; Owen *et al.* 2022a,b). Potential applications range from the creation of new kinds of commercially useful materials and uses in medical technology and pharmaceuticals. Three types of nanocellulose that have been studied extensively are cellulose nanocrystal (CNC), cellulose nanofiber (CNF), and bacterial nanocellulose (BNC) (Hubbe *et al.* 2017). Cellulose nanofiber has a greater proportion of amorphous structures than cellulose nanocrystals, so that it is more flexible. The diameter of cellulose nanofibrils is 1 to 100 nm, while the length is in the micrometer range (Abdul Khalil *et al.* 2014). Cellulose nanofibrils are a promising material for the manufacture of bio-composites because they have high strength, light weight, flexibility, and biodegradability (Liang *et al.* 2023). In addition, nanocellulosic materials have a large surface area; they bind to other compounds such as anti-bacterial and antioxidants (Bideau *et al.* 2017).

Nanofibers have limitless areas of application (Jiffrin *et al.* 2022) making them a very interesting area of research (Shen *et al.* 2020). The distinctive ordered architecture of natural cellulose having nanoscale fibers and crystals permits the preparation of the nano-components by chemical or mechanical methods, or a combination of both methods (Khan *et al.* 2022). The production of CNF is achieved by the reduction of the ordered structure of the bulk material through a breakdown process into individual nanofibers having very good crystallinity and low amorphous parts (Eichhorn *et al.* 2010).

Nanocellulose products have been prepared from various biomass sources such as wheat straw, sisal, hemp, soy hulls, palm oil, pineapple, wood, and kenaf (Faria *et al.* 2020; Franco-Urquiza and Rentería-Rodríguez 2021; Santos *et al.* 2021; Zhang *et al.* 2021; Pascoli *et al.* 2022; Zhang *et al.* 2022; Oliveira *et al.* 2023; Perera *et al.* 2023). Kenaf (*Hibiscus cannabinus* L., Malvaceae) is a common wild plant of tropical and subtropical Africa and Asia (Bourguignon *et al.* 2017). As the commercial use of kenaf continues to diversify from its historical role as a cordage crop (rope, twine, and sackcloth) to its various new applications including paper products (Azizi Mossello *et al.* 2010), building materials (Azzmi and Yatim 2010), absorbents (Tan *et al.* 2021), livestock feed (Kipriotis *et al.* 2015), and medical applications (Adnan *et al.* 2020), choices within the decision matrix will continue to increase and involve issues ranging from basic agricultural production methods to marketing of kenaf products (Bourguignon *et al.* 2017).

The kenaf stalk is 35% bark and 65% woody core by weight (Webber 1993). The kenaf plant consists of two distinct fibers. These are the outer layer (bast fiber), and a finer fiber in the core kenaf (Abdul Khalil *et al.* 2010; Silva *et al.* 2021). They have different lengths and chemical compositions. Apart from the chemical composition, the properties of kenaf (internal structure, microfibril angle, cell dimensions, and defects) are strongly influenced by many factors that may differ among different parts of the plant as well as among different plants (Silva *et al.* 2021). The kenaf core fibers are higher in holocellulose and lignin, 87.2% and 19.2%, respectively, while kenaf bast fiber is higher in α -cellulose. The α -cellulose content in bast fiber (55%) is higher than in the core (49%). A high α -cellulose content is believed to provide high strength fiber based end products (Al-Mamun *et al.* 2023).

The nanocellulose fibrils are isolated from the cellulosic fibers using various methods such as high-pressure homogenization, acid hydrolysis, *etc.* For example, Zaini *et al.* (2013) isolated kenaf-based CNC by using hydrolysis with H₂SO₄ or HCl. They obtained nano whiskers with average diameters and length of 3 nm and 100 to 500 nm, respectively. The homogenizers are used to delaminate the cell walls of the fibers and liberate the nanosized fibrils. Cellulose nanowhiskers, a more crystalline form of nanocellulose, are formed by the acid hydrolysis of native cellulose fibers using a concentrated inorganic salt, commonly sulfuric or hydrochloric acid. Song *et al.* (2018) extracted nanocellulose from kenaf using the combined microwave and chemical treatment showed an acicular morphology with nano-size fiber; it has a higher crystallinity but a bit lower thermal stability.

This work characterized kenaf bast nanofibers with X-ray diffraction (XRD), differential scanning calorimetry (DSC), scanning electron microscope (SEM), Fourier-transform infrared (FTIR) spectroscopy, and atomic force microscopy (AFM).

EXPERIMENTAL

Raw Materials

Kenaf was provided from National Fiber Council Indonesia (DSN) with KR 15 variety. Sodium hydroxide (NaOH), hydrogen peroxide (H₂O₂), anthraquinone (AQ), and magnesium sulphite (MgSO₄) were of analytical grade.

Preparation of Raw Materials

The kenaf bast was sun-dried until the moisture content was $\leq 12\%$. The dried kenaf bast was cut to the length of 2 to 3 cm, and then it was put through a hammer mill (S-tech 2- MHC, Indonesia) to get fine particles. The particles dried kenaf bast fibers were sieved through 100 mesh screens to eliminate the fine and coarse fibers.

Pulping Process

Pulping of kenaf bast was conducted based on the method by Fatriasari *et al.* (2015). Kenaf bast of 200-g dry weight and the cooking liquor (36.472g Na₂O, and 0.188g anthraquinone) with a ratio of 1:7 (chip/liquor) was added to a rotary digester (model GEC-P40306, India) and run for 2.5 h at 170 °C. The screened pulp was centrifugally dewatered, and the pulps were put for oven drying at 60 °C for 24 h.

Pulp Bleaching Process

A peroxide solution, at specific concentrations of 35 v/v%, was prepared as the bleaching solution. The weight ratio of the bleaching solution to slurry after alkaline process was 30:1. The bleaching process was carried out at 80 ± 2 °C and 200 rpm, and allowed a 2-h reaction time. The slurry was collected on a filter mesh and then thoroughly washed with distilled water. Finally, the damp bleached pulp was wrapped in a muslin cloth and centrifugally dewatered. The bleached pulp dried in an oven at 60 °C for 24 h.

Acid Hydrolysis Process

The acid hydrolysis treatments were carried out in an autoclave (Raypa AES-110 model) by adding 10 g of bleached pulp into 250 cm³ Erlenmeyer flasks and adding 100 cm³ of sulfuric acid (H₂SO₄ 60% wt) solution. The condition was conducted at temperatures 120 °C for 60 min. In this way, the solid–liquid ratio was kept at a constant value of 10. Flasks were sealed with fatty cotton wrapped in sterile gauze and covered, at the top, with aluminum foil. Each acid solution was mixed with fragmented bleached pulp by slight agitation, and the system was subjected to autoclave thermal processing. The acid was removed by centrifugation using an Eppendorf Centrifuge (model 5804/5804 R, Germany) at a rotating speed of 6500 rpm for 5 min.

Scanning Electron Microscope (SEM)

Scanning electron microscopy (SEM) was used to identify morphological changes on kenaf bast fibers surface. Longitudinal segments of raw kenaf bast, unbleached pulp, and bleached pulp were mounted in an aluminium substrate at an angle of 45° and coated with gold with thickness of approximately 90 Å. Surface morphology of the absorbents was identified by SEM (model EVO MA10, Carl-Zeiss SMT, Germany) in order to understand the morphology of the kenaf fibers at an accelerating voltage of 20 KV.

Fourier-transform Infrared (FTIR) Spectroscopy

The FT-IR microscope (model IS10 Nicolet, Thermo Scientific, USA) was used to obtain the spectra of fiber kenaf bast. OPUS software was used for collecting the spectrum in the mid infrared range of 400 to 400 cm^{-1} with a resolution of 4 cm^{-1} . The spectra were used to determine changes in functional groups that may have been caused by treatments. Each sample was scanned for three trials and an average spectrum was obtained. After that, the spectra were smoothed automatically using OPUS software to enhance the FT-IR spectrum quality.

Differential Scanning Calorimetry (DSC)

Differential scanning calorimetry analysis was operated by using DSC furnace model Perkin- Elmer DSC- 821, USA. The samples with the weight of 2.30 mg were used and analyzed dynamically at a heating rate of 5.4 $^{\circ}\text{C}/\text{min}$ using N_2 . The maximum temperature was set up to 600 $^{\circ}\text{C}$ under a nitrogen atmosphere.

X-ray Diffraction (XRD)

A Phillips PW 1840 X-ray Diffractometer was used for obtaining the X-ray diffractograms. Nickel filtered $\text{CuK}\alpha$ radiations at 35 KV ($\text{K}\alpha = 1.54 \text{ \AA}$) with the accelerating voltage of 40 kV, and current of 25 mA were employed. The samples were scanned in the range from 5 to 90 $^{\circ}$ of 2θ with a step size of 0.05 $^{\circ}$. Further, the crystallinity index (CI) was determined with the ratio of the area of all crystalline peaks (A_{cr}) to the total area (A_{total}) (Park *et al.* 2010).

$$CI = A_{cr} / A_{total} \quad (1)$$

Atomic Force Microscopy (AFM)

The atomic force microscopy (AFM) model (XE-70 Park System, Germany) was used to analyze morphology of the obtained nanofibers by acid hydrolysis treatment. The sample was diluted to the desired concentration using distilled water then sonicated to obtain good dispersion. A drop of suspension was deposited on fresh cleaved mica and left to dry in a desiccator with silica gel for 12 h. AFM analysis were performed using a Digital III- Instrument under atmospheric conditions at 25 $^{\circ}\text{C}$.

RESULTS AND DISCUSSION

Morphology of the Treated and Untreated Kenaf Bast

The morphology of the treated and untreated kenaf bast fiber, unbleached pulp and bleached pulp was studied using SEM. Figure 1 contains SEM micrographs of the raw kenaf bast, treated and untreated. The alkaline retting treatment liberated single fiber from the fiber bundles of the raw kenaf bast fiber. The bleached fiber morphology was altered little by the bleaching treatment.

Figure 1(a) shows that the raw kenaf bast fiber bundle composed of individual fiber linked with lignin. The diameter of the raw kenaf bast fiber was 30 μm . The surfaces of the raw kenaf fibers retrieved from water retting did not show any mechanical damages, despite the presence of lignin. These findings are consistent with previous reports of retted kenaf fibers (Nie *et al.* 2020; Rozyanty *et al.* 2021). Figure 1(b) and 1(c) show the structure of the fiber after pulping and bleaching processes. The SEM images can also reveal a clean

surface and finer possess of the fiber by the end of the pulping and bleaching processes. These processes separate the fiber bundle into individual fibers and cause a significant decrease in their diameter. The unbleached pulp fiber diameter is 12 μm , and the diameter for bleached pulp is 9 μm . The surface and diameter of the natural fibers were aligned with the adjacent lignin, and their elimination through the pulping and bleaching process reduced its dimensions and improved fineness (Beltran *et al.* 2002).

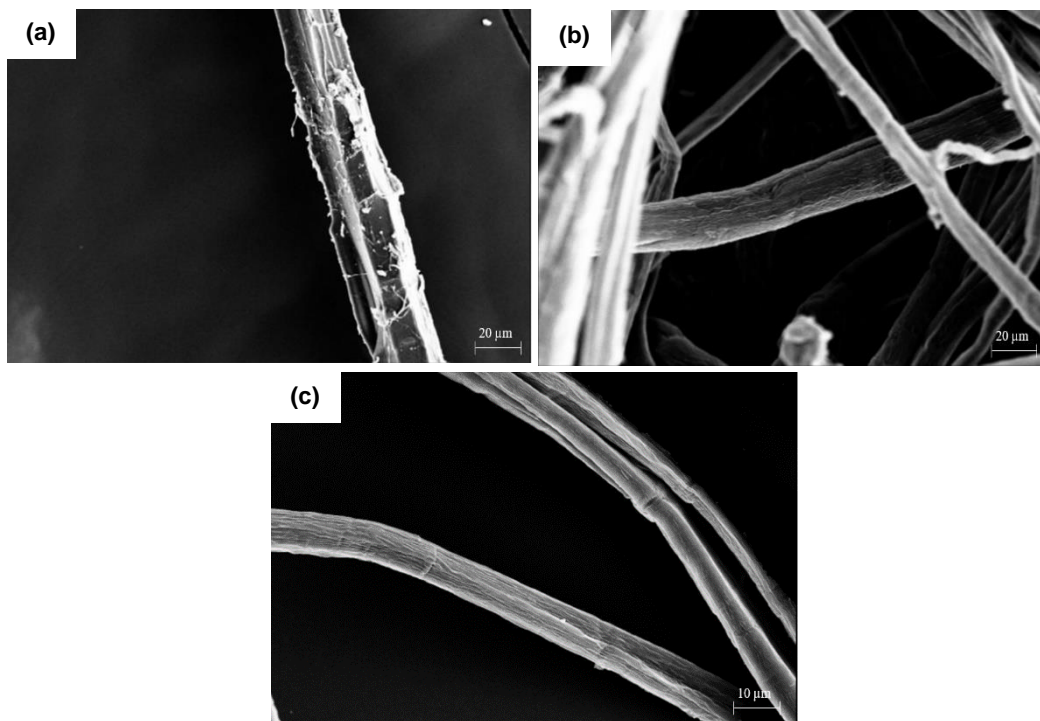


Fig. 1. SEM images of (a) raw fiber, (b) unbleached pulp, and (c) bleached pulp

FTIR Spectroscopy

FTIR spectroscopy was used to identify the functional groups on the raw kenaf bast, unbleached pulp and bleached pulp. The main differences in FTIR spectra can be seen in Fig. 2. Some differences were apparent in the magnitudes of bands in the FTIR spectrum of kenaf bast fiber, unbleached pulp, and bleached pulp. The broad and dominant peaks around 3400 to 3300 cm^{-1} were associated with the stretching of O-H groups, including intramolecular and intermolecular hydrogen bonds (Wang *et al.* 2017; Lu *et al.* 2022). The peak located at 1737.18 cm^{-1} (Fig. 2a) in the raw kenaf bast was assigned to the C=O stretching of the acetyl group in hemicelluloses (Hossain *et al.* 2022). In the raw kenaf bast, the peak at 1249.4 cm^{-1} was associated to the C-O stretching of the aryl group in lignin (Zarina and Ahmad 2015). However, the lowest O-H absorption was seen in the treatment with active alkali and sulfidity (bleached pulp). In addition, a decrease in the intensity of O-H stretching vibration also indicated partial acetylation of cellulose (Fan *et al.* 2013). The change of O-H stretching vibrations was dependent on the extent to which the chemical treatment altered inter- and intra-molecular hydrogen bonding in polysaccharides (Martín-Alfonso *et al.* 2018). Furthermore, the disappearance of this peak (C-O stretching) occurred in the unbleached and bleached pulp due to the removal of lignin after the chemical treatments (Wang *et al.* 2018). The content of carboxyl groups in pulp first increases and then decreases in bleached pulp (Mingfu *et al.* 2020).

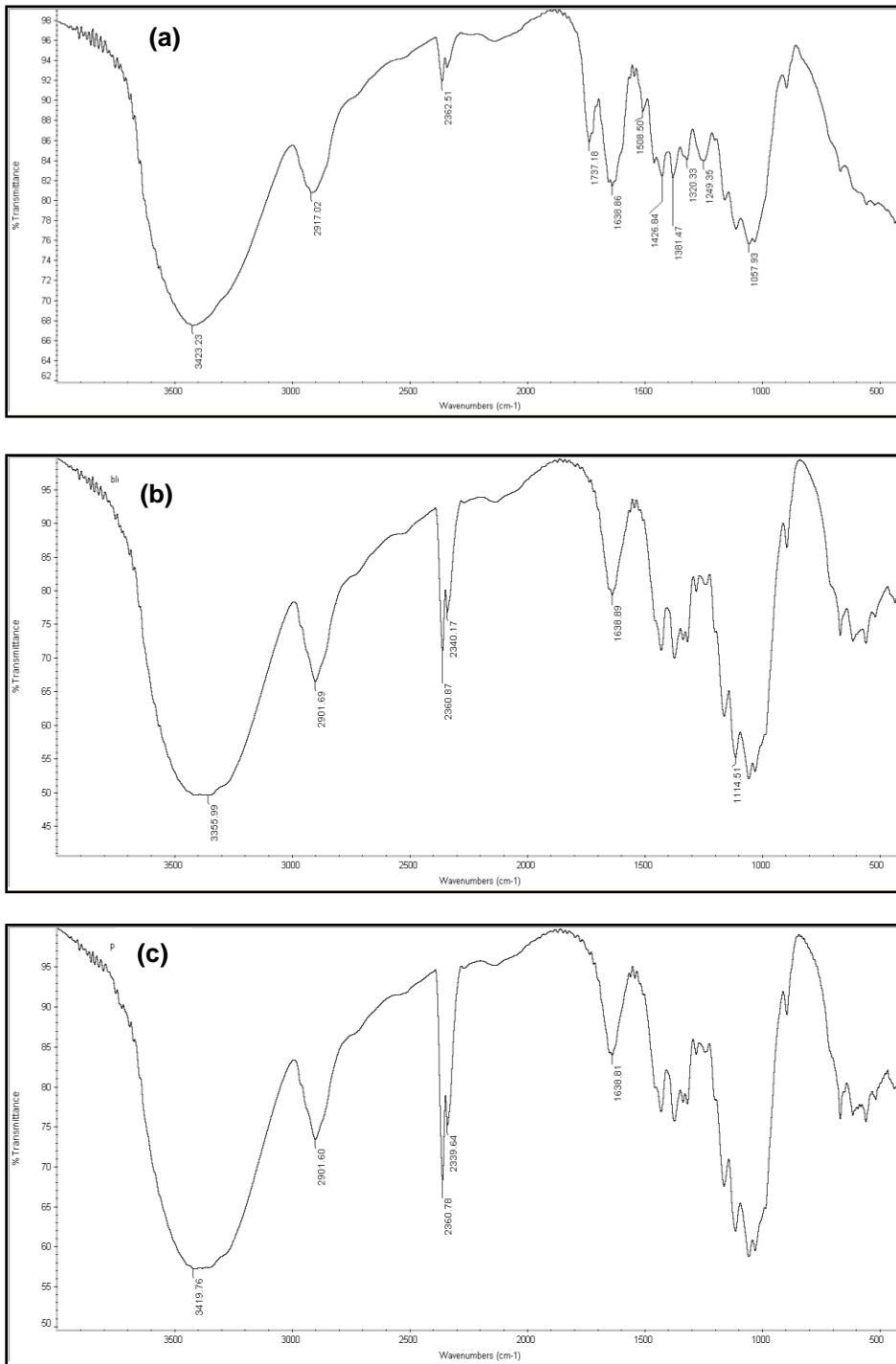


Fig. 2. FTIR spectra of the kenaf bast fiber. (a) the raw kenaf bast, (b) the unbleached pulp, (c) the bleached pulp

The peaks observed in the ranges of 1420 to 1430 cm^{-1} and 1330 to 1380 cm^{-1} in all spectra were attributed to the symmetric bending of CH_2 and the bending vibrations of the C-H and C-O groups of the aromatic rings polysaccharides, respectively (Carrillo *et al.*, 2018). After treatment (Fig. 2b, 2c) absorption peaks of $\sim 1030 \text{ cm}^{-1}$ of the kenaf bast sample, which corresponded to the C-O-C vibration found in cellulose and hemicelluloses,

as well as the C-C stretching vibration or COH bending seen in hemicellulose (Zhao *et al.* 2020), were significantly greater than those of the raw kenaf bast. By comparing the spectrum before and after the chemical treatment of the kenaf bast used, it was observed that the intensity of the typical peak of C-H groups in the cellulose at 2901.69 cm^{-1} was decreased (Tang *et al.* 2015). The obtained results confirmed that the effect of chemical treatment using a low concentration of NaOH on the degradation of coating substances (lignin, hemicellulose, and pectin) could influence the size of cellulosic fibers relative to the initial length (Nurazzi *et al.* 2021).

Crystallinity

Crystallinity is an important factor to evaluate the cellulose properties of biomass after pretreatment. It was obtained from the 2θ peak in XRD diffractograms. The X-ray diffraction (XRD) spectra of the raw kenaf bast fiber, unbleached pulp, and bleached pulp are shown in Fig. 3. As shown in the figure, the XRD diffraction pattern of kenaf bast fiber samples showed two dominant peak intensities at the diffraction angles (2θ) of $\sim 15.81^\circ$, and $\sim 22.51^\circ$, while the low intensity peaks can be assigned to other elements present in the kenaf bast fiber. A peak at around $\sim 22.51^\circ$ (2θ) showed the crystalline peak of cellulose (Trilokesh and Uppuluri 2019; Yi *et al.* 2020). Meanwhile, the broad peak at 2θ around $\sim 15.81^\circ$ represented the amorphous material of lignocellulose, such as amorphous cellulose, hemicellulose, and lignin (Singh *et al.* 2017). The crystallinity index (CI) of kenaf bast fiber was calculated from XRD intensity data using peak deconvolution method were 49.28%, 59.10%, and 63.54% for the raw, unbleached pulp, and bleached pulp, respectively.

Based on the samples of unbleached pulp and bleached pulp there was an increase of crystallinity index (Fig. 3b, and c). The higher crystallinity index on bleached pulp sample caused by active alkali gave an increasing α -cellulose content (Solihat *et al.* 2017). The fiber crystallinities gradually increased at each stage of the process. Alkaline retting removes lignin and hemicelluloses, so that the percentage of the crystalline regions in cellulose increased. Hydrogen peroxide bleaching accelerated the cleavage of the cellulose molecular chains within the amorphous regions, resulting in the further increase of the crystallinity of the bleached first (Shi *et al.* 2011). During the bleaching treatment with the existence of alkali, the cellulose may be oxidized, and degradation of cellulose would have occurred (Qu *et al.* 2010). In addition, the remaining lignin was degraded by hydrogen peroxide and removed during bleaching. The chromophore structures of lignin were destroyed by oxidizing the carbonyl structure and quinoid structure of lignin side chain during H_2O_2 bleaching (Li *et al.* 2020).

Thermal Analysis

The DSC thermograms of kenaf bast fiber, unbleached pulp and bleached pulp are shown in Fig. 4. The samples were heated from 25 to 450 °C over 45 min to measure the melting temperature.

DCS was carried out to determine the thermal behaviour of the fibers. DSC analysis also enables the identification to be made of chemical activity occurring in the fibers as the temperature is increased (Agung *et al.* 2011). Figure 4a shows the DSC curve for raw kenaf bast fiber. The T_g of raw kenaf bast fiber was clearly observed at two peaks, peak 1 at 163.8 °C and 170.5 °C, peak 2 at 183.3 °C and 193.2 °C representing onset and midpoint temperature, respectively. In this DSC curve, the hemicellulose exhibited an exothermic peak at 165.3 °C (peak 3) with an enthalpy value of 16.5 J/g. Its amorphous structure broke

down and formed residual char, whereas the thermal degradation of cellulose was associated with a peak at 185.9 °C (peak 4) with an associated enthalpy of 16.6 J/g.

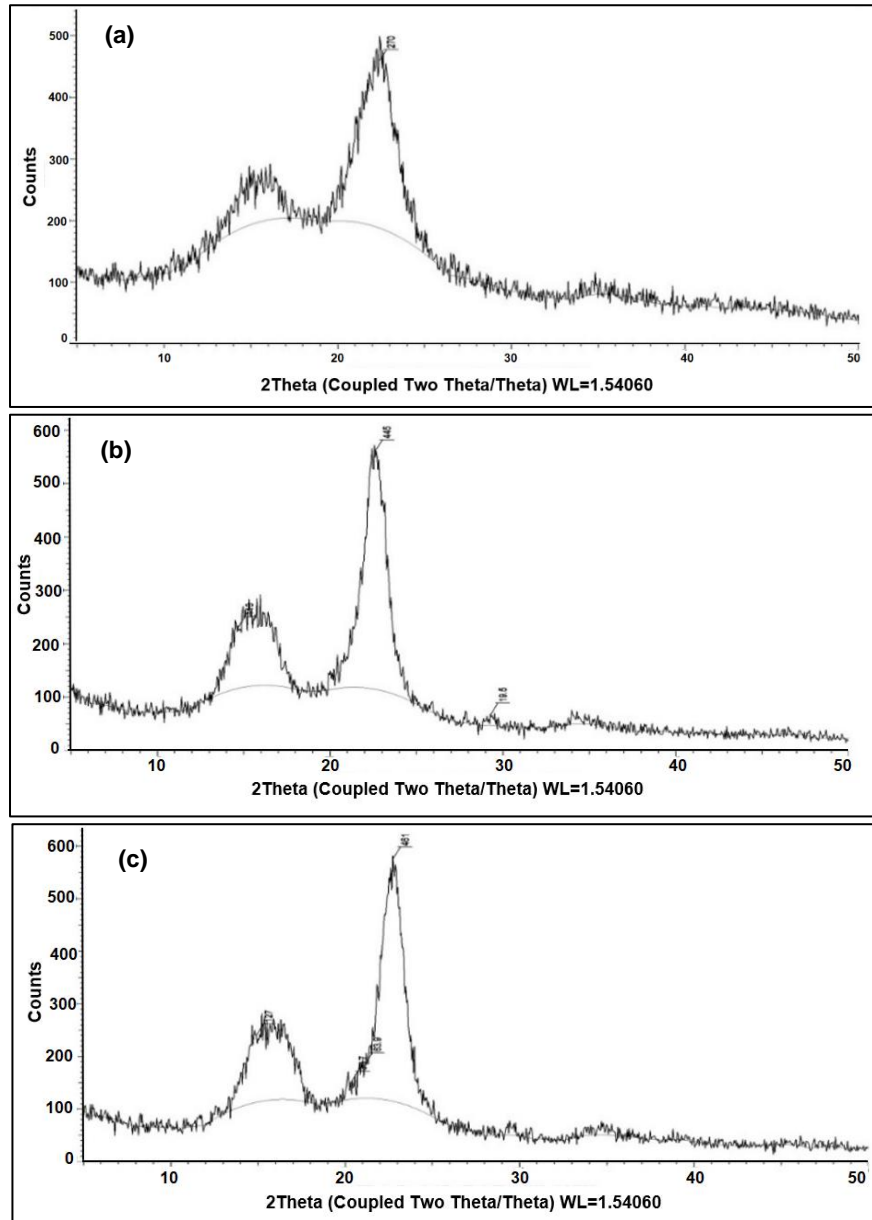


Fig. 3. X-ray diffraction spectra. (a) the raw kenaf fiber, (b) unbleached pulp, and (c) bleached pulp

T_g is manifested by a drastic change in the base line, indicating the beginning of the decomposition of cellulose and hemicellulose and lignin, which takes longer to start the decomposition (Silva *et al.* 2016). Differential thermal analysis curves of raw kenaf bast fiber show that a broad endotherm observed in the temperature range of 150 to 175 °C, its indicates presence of water molecules in the fibers. This endothermic peak above 100 °C were observed, which is due to the dehydration of the water stored in the fiber (Shahinur *et al.* 2020).

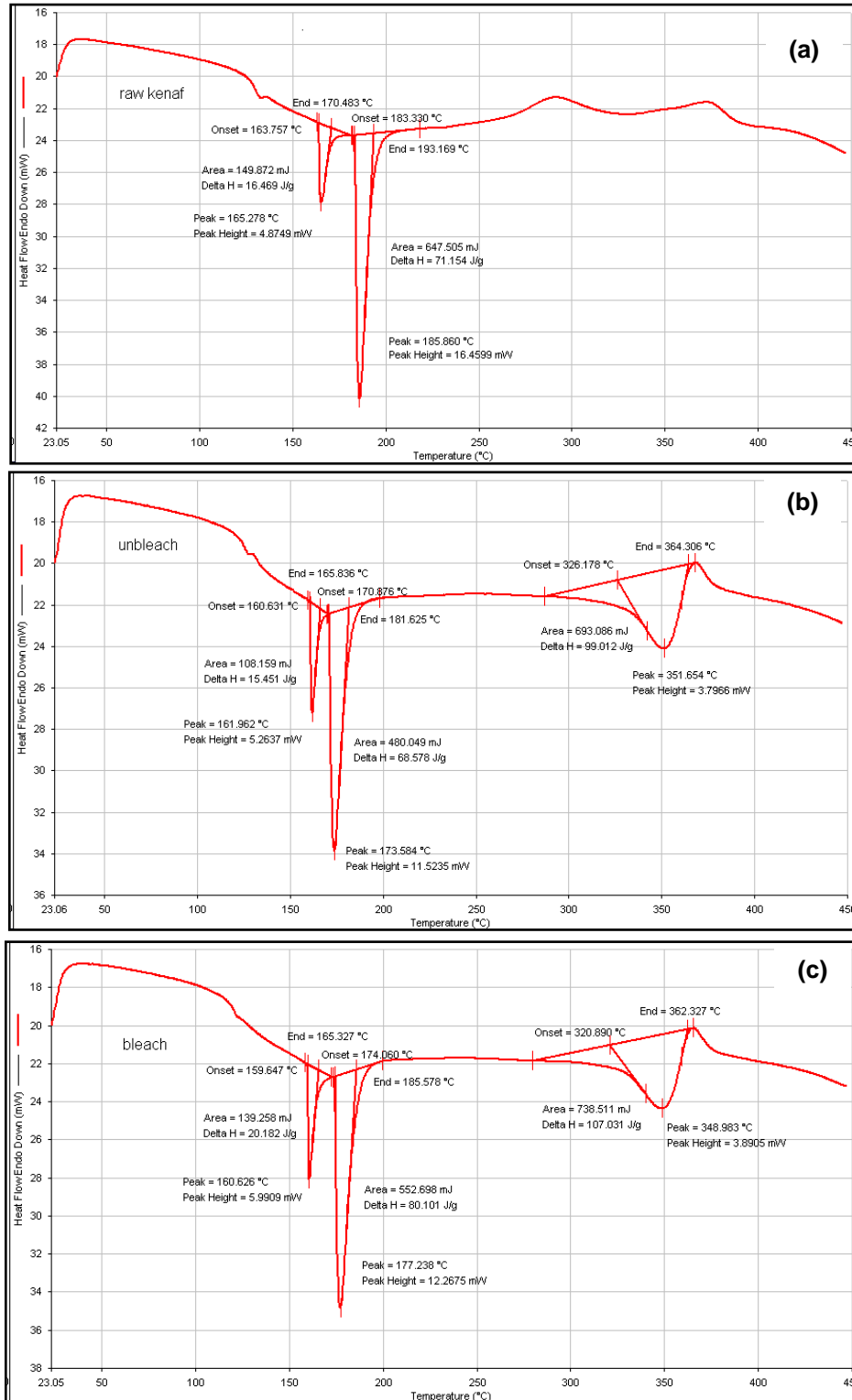


Fig. 4. DSC thermograms. (a) the raw kenaf fiber, (b) unbleached pulp, and (c) bleached pulp

The heating thermograms of kenaf bast fiber after treatment (unbleached pulp and bleached pulp) represent the one peak in the endothermic due to crystallization state. The first peaks of treated kenaf bast fiber were at 162.0 °C (unbleached pulp) and 160.6 °C (bleached pulp), respectively. The first endothermic peak, which can be attributed to the

loss of water was observed in the range of 150 to 175 °C for kenaf bast fiber, whereas for the unbleached and bleached pulp sample the first endothermic peak was observed within the range of 150 to 160 °C. In cellulose fibres, lignin degrades at a temperature around 200 °C, while the other polysaccharides such as cellulose degrade at higher temperatures (Bharath *et al.* 2020). As can be seen from DSC thermograms, it is evident that the peak between 250 to 350 °C belongs to cellulose melting or decomposition. This peak does not show any endothermic or exothermic reactions and are representative of the highest stable state of the kenaf bast fibers (Lemita *et al.* 2022). The peaks between 100 to 200 °C are simply dehydration. Although it should be a single peak, the multiplicity may be because of some constituents like some waxy materials. Therefore these exothermic peaks, which were higher than 200 °C, indicate the decomposition temperatures of the cellulose in the fibers.

Atomic Force Microscopy (AFM) Analysis

Figure 5 shows an AFM image of cellulose whiskers, which is another term meaning CNC. The surface morphology of CNC appeared as rod-shaped fragments, which were overlapping each other in the image to form larger aggregates, showing similar diameters of the particles (Fig. 5, left). The surface morphology displayed the broadening effect and possibly agglomeration of the cellulose whiskers. The cellulose whiskers are known to have high colloidal stability, which is due to the electrostatic repulsion between the sulfate group-grafted surfaces resulting from the sulfuric acid treatment (Gousse *et al.* 2002). The subsequent peroxide bleaching process yielded crude cellulose which contained amorphous and crystalline domain. Furthermore, during acid hydrolysis the H⁺ ion would penetrate the cellulose chains and interact with the cellulose.

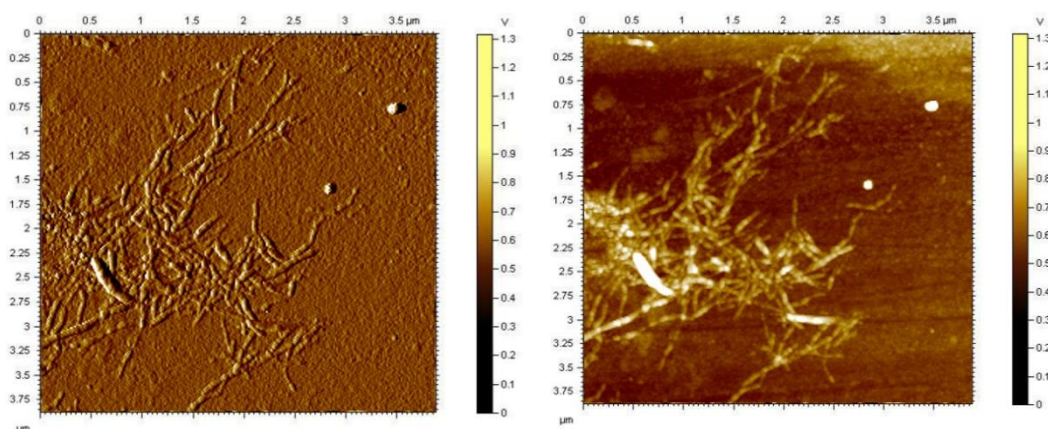


Fig. 5. AFM image of cellulose whiskers

Most of the CNC crystals finally obtained had the length of 300 to 450 nm and diameter of 30 nm (Fig. 5, right). The AFM images of the nanocellulose obtained from kenaf bast fiber clearly showed the presence of needle-shaped CNC samples finally after acid hydrolysis at optimal condition (Masoudzadeh *et al.* 2019). This result is favored by another study (Lu and Hsieh 2012), where the diameter was around 50 nm. Hence, acid hydrolysis treatment with concentration and reaction time decreased the crystals' diameter.

CONCLUSIONS

1. After bleaching, the diameter of kenaf bast fiber decreased, which was attributed to the fact that such processes separate the fiber bundle to individual fibers.
2. The Fourier transform infrared (FTIR) results showed the disappearance of spectral peaks in the unbleached and bleached pulps due to removal of lignin in the course of the chemical treatment.
3. X-Ray diffraction analysis showed that the raw kenaf bast fiber, unbleached and bleached pulp crystallinities gradually increased at each stage of process. Alkaline retting removed lignin and hemicelluloses so that the percentage of the crystalline region in cellulose increased.
4. In differential scanning calorimetry (DSC) thermograms, it was evident that the peak between 250 and 350 °C belonged to cellulose melting or decomposition, while the peak between 100 and 200 °C was simply dehydration. Although it should be a single peak, it appeared as a multiple peak, which may be because of some waxy constituents. The exothermic peaks, which were higher than 200 °C, indicate the decomposition temperature of the cellulose in the fiber. After getting the micrometer result, acid hydrolysis was conducted to produce nanocellulose.
5. Atomic force microscopy of the kenaf bast-based nano-whiskers showed that the diameter of their crystals was approximately 30 nm. The CNCs were similar to those of other natural fiber-based CNCs, but their nanoscale structures diverged.

ACKNOWLEDGMENTS

The authors thank the Ministry of Education, Culture, Research and Technology (KEMENDIKBUDRISTEK), Republic of Indonesia, for providing Research Grant " Basic Research Scheme" No. 110/E5/PG.02.00.PL/2023. The authors also thank the Integrated Laboratory of Bioproduct (iLaB) of Research Center for Biomass and Bioproducts, National Research and Innovation Agency (BRIN), Indonesia, for providing the facilities for testing.

REFERENCES CITED

- Abdul Khalil, H. P. S., Ireane Yusra, A.F., Bhat, A.H., and Jawaid, M. (2010). "Cell wall ultrastructure, anatomy, lignin distribution, and chemical composition of Malaysian cultivated kenaf fiber," *Ind Crops Prod.* 31(1), 113-121. DOI: 10.1016/j.indcrop.2009.09.008
- Abdul Khalil, H. P. S., Davoudpour, Y., Islam, M. N., Mustapha, A., Sudesh, K., Dungani, R., and Jawaid, M. (2014). "Production and modification of nanofibrillated cellulose using various mechanical processes: A review," *Carbohydr. Polym.* 99, 649-665. DOI: 10.1016/j.carbpol.2013.08.069
- Achukwu, E. O., Odey J. O., Owen, M. M., Lawal N., Oyilagu G. A., and Adamu A. I. (2022). "Physical and mechanical properties of flamboyant (*Delonix regia*) pod-filled polyester composites," *Heliyon* 8(1), e08724. DOI: 10.1016/j.heliyon.2022.e08724

- Adnan, Md., Oh, K. W., Azad, O. K., Shin, M. H., Wang, M. H., and Cho, D. H. (2020). "Kenaf (*Hibiscus cannabinus* L.) leaves and seed as a potential source of the bioactive compounds: Effects of various extraction solvents on biological properties," *Life* 10(10), 223. DOI: 10.3390/life10100223
- Agung, E. H., Sapuan, S. M., Megat Ahmad, M. M. H., Zaman, H. M. D. K., and Mustofa, U. (2011). "Differential scanning calorimetry (DSC) analysis of abaca fibre (*Musa Textile Nee*) reinforced high impact polystyrene (HIPS) composites," *Adv. Mater. Res.* 295-297, 929-933. DOI: 10.4028/www.scientific.net/AMR.295-297.929
- Al-Mamun, Md., Rafii, M. Y., Misran, A.B., Berahim, Z., Ahmad, Z., Khan, M.H., Oladosu, Y., and Arolu, F. (2023). "Kenaf (*Hibiscus Cannabinus* L.): A promising fiber crop with potential for genetic improvement utilizing both conventional and molecular approaches," *J. Natur. Fibers* 20(1), 2145410. DOI: 10.1080/15440478.2022.2145410
- Azizi Mossello, A., Harun, J., Resalati, H., Ibrahim, R., Fallah Shmas, S. R., and Paridah Md. T. (2010). "New approach to use of kenaf for paper and paperboard production," *BioResources* 5(4), 2112-2122. DOI: 10.15376/biores.5.4.2112-2122
- Azzmi, M. N., and Yatim, J. M. (2010). "Kenaf fibrous concrete: Mechanical properties with different fiber volume fraction," *Int. J. Adv. Sci. Eng. Inf. Technol.* 8(4), 1036-1042.
- Beltran, R., Hurren, C. J., Kaynak, A., and Wang, X. (2002). "Correlating the fineness and residual gum content of degummed hemp fibres," *Fibers Polym.* 3, 129-133. DOI: 10.1007/BF02912656
- Bharath, K. N., Madhu, P., Gowda, T. G. Y., Sanjay, M. R., Kushvaha, V., and Siengchin, S. (2020). "Alkaline effect on characterization of discarded waste of *Moringa oleifera* fiber as a potential eco-friendly reinforcement for biocomposites," *J. Polym. Environ.* 28, 2823-2836. DOI:10.1007/s10924-020-01818-4
- Bideau, B., Bras, J., Adoui, N., Loranger, E., and Daneault, C. (2017). "Polypyrrole/nanocellulose composite for food preservation: Barrier and antioxidant characterization," *Food Packag. Shelf Life.* 12, 1-8. DOI: 10.1016/j.fpsl.2017.01.007
- Bourguignon, M., Archontoulis, S., Moore, K., Lenssen A. (2017). "A model for evaluating production and environmental performance of kenaf in rotation with conventional row crops," *Ind. Crops Prod.* 100, 218-227. DOI: 10.1016/j.indcrop.2017.02.026
- Carrillo, I., Mendonça, R. T., Ago, M., and Rojas, O. J. (2018). "Comparative study of cellulosic components isolated from different *Eucalyptus* species," *Cellulose* 25, 1011-1029. DOI: 10.1007/s10570-018-1653-2
- Hubbe, M. A., Ferrer, A., Tyagi, P., Yin, Y., Salas, C., Pal, L., and Rojas, O. J. (2017). "Nanocellulose in thin films, coatings, and plies for packaging applications: A review," *BioResources* 12(1), 2143-2233. DOI: 10.15376/biores.12.1.2143-2233
- Eichhorn, S. J., Dufresne, A., Aranguren, M., Marcovich, N. E., Capadona, J. R., Rowan, S. J., and Peijs, T. (2010). "Review: current international research into cellulose nanofibers and nanocomposites," *J. Mater. Sci.* 45(1), 1-33. DOI: 10.1007/s10853-009-3874-0
- Fan, G., Wang, M., Liao, C., Fang, T., Li, J., and Zhou, R. (2013). "Isolation of cellulose from rice straw and its conversion into cellulose acetate catalyzed by phosphotungstic acid," *Carbohydr. Polym.* 94, 71-76. DOI: 10.1016/j.carbpol.2013.01.073
- Faria, L. U. S., Pacheco, B. J. S., Oliveira, G. C., and Silva, J. L. (2020). "Production of cellulose nanocrystals from pineapple crown fibers through alkaline pretreatment and

- acid hydrolysis under different conditions,” *J. Mater. Res. Technol.* 9(6), 12346-12353. DOI: 10.1016/j.jmrt.2020.08.093
- Fatriasari, W., Suprianto, A., and Iswanto, A.H. (2015). The kraft pulp and paper properties of sweet sorghum bagasse (*Sorghum bicolor* L. Moench). *J. Eng. Technol. Sci.* 47, 149-159. DOI: 10.5614/j.eng.technol.sci.2015.47.2.4
- Franco-Urquiza, E., and Rentería-Rodríguez, A. (2021). “Effect of nanoparticles on the mechanical properties of kenaf fiber-reinforced bio-based epoxy resin,” *Text. Res. J.* 1(11-12), 313-1325. DOI: 10.1177/0040517520980459
- Gousse, C., Chanzy, H., Excoffier, G., Soubeyrand, L., and Fleury, E. (2002). “Stable suspensions of partially silylated cellulose whiskers dispersed in organic solvents,” *Polymers.* 3(9), 2645-2651. DOI: 10.1016/S0032-3861(02)00051-4
- Hossain, M. M., Subbiah, V. K., and Siddiquee, S. (2022). “Augmented retting effect on kenaf fibers using alkalophilic pectinase-producing bacteria in combination with water solvents,” *Appl. Sci.* 12, 7136. DOI: 10.3390/app12147136
- Jiffrin, R., Abd Razak, S. I., Jamaludin, M. I., Hamzah, A. S. A., Mazian, M. A., Jaya, M. A. T., Nasrullah, M. Z., Majrashi, M., Theyab, A., Aldarmahi, A. A., Awan, Z., Abdel-Daim, M. M., and Azad, A. K. (2022). “Electrospun nanofiber composites for drug delivery: A review on current progresses,” *Polymers* 14, 3725. DOI: 10.3390/polym14183725
- Khan, Y., Sadia, H., Ali Shah, S. Z., Khan, M. N., Shah, A. A., Ullah, N., Ullah, M. F., Bibi, H., Bafakeeh, O. T., Khedher, N. B., Eldin, S. M., Fadhl, B. M., and Khan, M. I. (2022). “Classification, synthetic, and characterization approaches to nanoparticles, and their applications in various fields of nanotechnology: A review,” *Catalysts* 12, 1386. DOI: 10.3390/catal12111386
- Kipriotis, E., Heping, X., Vafeiadakis, T., Kiprioti, M., and Alexopoulou, E. (2015). “Ramie and kenaf as feed crops,” *Ind. Crops Prod.* 68: 126-130. DOI: 10.1016/j.indcrop.2014.10.002
- Mingfu, Li, M., Yin, J., Hu, L., Chenb, S., Mina, D., Wang, S., and Luo, L. (2020). “Effect of hydrogen peroxide bleaching on anionic groups and structures of sulfonated chemo-mechanical pulp fibers,” *Colloids Surf. A: Physicochem. Eng.* 585, 124068. DOI: 10.1016/j.colsurfa.2019.124068
- Lemita, N., Dighboudj, S., Rokbi, M., Rekbi, F. M. L., and Halimi, R. (2022). “Characterization and analysis of novel natural cellulosic fiber extracted from *Strelitzia reginae* plant,” *J. Compos. Mater.* 56(1). 99-114. DOI: 10.1177/00219983211049285
- Liang, D., Liu, W., Zhong, T., Liu, H., Dhandapani, R., Li, H., Wang, J., and Wolcott, M. (2023). “Nanocellulose reinforced lightweight composites produced from cotton waste via integrated nanofibrillation and compounding,” *Sci. Rep.* 13, 2144. DOI: 10.1038/s41598-023-29335-z
- Lu, P., and Hsieh, Y. L. (2012). “Preparation and characterization of cellulose nanocrystals from rice straw,” *Carbohydr. Polym.* 87, 564-573. DOI: 10.1016/j.carbpol.2011.08.022
- Lu, S., Ma, T., Hu, X., Zhao, J., Liao, X., Song, Y., and Hu, X. (2022). “Facile extraction and characterization of cellulose nanocrystals from agricultural waste sugarcane straw,” *J. Sci. Food Agric.* 102, 312-321. DOI: 10.1002/jsfa.11360
- Martín-Alfonso, J.E., López-Beltrán, F., Valencia, C., and Franco, J.M. (2018). “Effect of an alkali treatment on the development of cellulose pulp-based gel-like dispersions in vegetable oil for use as lubricants,” *Tribol. Inter.* 123, 329-336. DOI:

10.1016/j.triboint.2018.02.027

- Masoudzadeh, F., Jamshidi, M., and Fasihi, M. (2019). "Preparation and application of cellulose nano whiskers (CNWs) in engineered cementitious composites," *J. Build. Eng.* 21, 213-221. DOI: 10.1016/j.job.2018.10.020
- Nie, K., Liu, B., Zhao, T., Wang, H., Song, Y., Ben, H., Ragauskas, A. J., Han, G., Jiang, W. (2020). "A facile degumming method of kenaf fibers using deep eutectic solution," *J. Nat. Fibers.* 19, 1115-1125. DOI: 10.1080/15440478.2020.1795778
- Nurazzi, N. M., Asyraf, M. R. M., Rayung, M., Norrahim, M. N. F., Shazleen, S. S., Rani, M. S. A., Shafi, A. R., Aisyah, H. A., Radzi, M. H. M., Sabaruddin, F. A., Ilyas, R. A., Zainudin, E. S., and Abdan, K. (2021). "Thermogravimetric analysis properties of cellulosic natural fiber polymer composites: A review on influence of chemical treatments," *Polymers* 13, 2710. DOI: 10.3390/polym13162710
- Oliveira, G. R., Andrade, C., Bez, I. C. C., Melo, A. D. B., Almeida, V. V., Magalhães, W. L. E., Weber, S. H., Sotomaior, C. S., Luciano, F. B., and Cost, L. B. (2023). "Inclusion of soybean hulls (*Glycine max*) and pupunha peach palm (*Bactris gasipaes*) nanofibers in the diet of growing rabbits: Effects on zootechnical performance and intestinal health," *Animals* 13, 192. DOI: 10.3390/ani13020192
- Owen, M. M., Achukwu, E. O., and Akil, H. M. (2022a). "Preparation and mechanical characterizations of water hyacinth fiber based thermoset epoxy composite," *J. Nat. Fib.* 19(16), 13970 -13984. DOI: 10.1080/15440478.2022.2113850
- Owen, M. M., Achukwu, E. O., Akil, H. M., Romli, A. Z., and Ishiaku, U. S. (2022b). "Characterization of recycled and virgin polyethylene terephthalate composites reinforced with modified kenaf fibers for automotive application," *Polym. Compos.* 43(11), 7724-7738. DOI: 10.1002/pc.26866
- Park, S., Baker, J., Himmel, M., Parilla, P., and Johnson, D. (2010). "Cellulose crystallinity index: Measurement techniques and their impact on interpreting cellulose performance," *Biotechnol. Biofuels.* 3(1), 3-11. DOI: 10.1186/1754-6834-3-10
- Pascoli, D. U., Dichiara, A., Roumeli, E., Gustafson, R., and Bura, R. (2022). "Lignocellulosic nanomaterials production from wheat straw via peracetic acid pretreatment and their application in plastic composites," *Carbohydr. Polym.* 295, 119857. DOI: 10.1016/j.carbpol.2022.119857
- Perera, U. P., Foo, M. L., and Chew, I. L. M. (2023). "Synthesis and characterization of lignin nanoparticles isolated from oil palm empty fruit bunch and application in biocomposites," *Sustain. Chemis. Clim. Act.* 2, 100011. DOI: 10.1016/j.scca.2022.100011
- Qu, L., Zhu, S., Liu, M., and Wang, S. (2010). "The mechanism and technology parameters optimization of alkali-H₂O₂ one-bath cooking and bleaching of hemp," *J. Appl. Polym. Sci.* 97, 2279-228. DOI: 10.1002/app.22024
- Rozyanty, A., Zhafer, S., Shayfull, Z., Nainggolan, I., Musa, L., and Zheing, L. (2021). "Effect of water and mechanical retting process on mechanical and physical properties of kenaf bast fiber reinforced unsaturated polyester composites," *Compos. Struct.* 257, 113384. DOI: 10.1016/j.compstruct.2020.113384
- Santos, R. D., Thomas, S., Ferreira, S. R., Silva, F. A., Combariza, M. Y., Blanco-Tirado, C., Ovalle-Serrano, S. A., Souza Jr, F. G., Oliveira, G. E., and Toledo Filho, R. G. (2021). "Molecular grafting of nanoparticles onto sisal fibers - adhesion to cementitious matrices and novel functionalities," *J. Mol. Struct.* 1234, 130171. DOI: 10.1016/j.molstruc.2021.130171
- Shahinur, S., Hasan, M., Ahsan, Q., and Haider, J. (2020). "Effect of chemical treatment

- on thermal properties of jute fiber used in polymer composites,” *J. Compos. Sci.* 4(3), 132. DOI: 10.3390/jcs4030132
- Shen, R., Xue, S., Xu, Y., Liu, Q., Feng, Z., Ren, H., Zhai, H., and Kong, F. (2020). “Research progress and development demand of nanocellulose reinforced polymer composites,” *Polymers* 12, 2113. DOI: 10.3390/polym12092113
- Shi, J., Shi, S. Q., Barnes, H. M., Horstemeyer, M., Wang, J., and Hassan, E. B. M. (2011). “Kenaf bast fibers-Part I: Hermetical alkali digestion,” *Inter. J. Polym. Sci.* 212047, 1-8. DOI: 10.1155/2011/212047
- Silva, T.T.d., Silveira, P.H.P.M.d., Ribeiro, M.P., Lemos, M.F., da Silva, A.P., Monteiro, S.N., and Nascimento, L.F.C. (2016). “Thermal and chemical characterization of kenaf fiber (*Hibiscus cannabinus*) reinforced epoxy matrix composites. *Polymers*. 13. DOI: 10.3390/polym13122016
- Silva, T. T. d., Silveira, P. H. P. M.d., Ribeiro, M. P., Lemos, M. F., da Silva, A. P., Monteiro, S. N., and Nascimento, L. F. C. (2021). “Thermal and chemical characterization of kenaf fiber (*Hibiscus cannabinus*) reinforced epoxy matrix composites,” *Polym.* 13, 2016. DOI: 10.3390/polym13122016
- Singh, Y.D., Mahanta, P., and Bora, U. (2017). “Comprehensive characterization of lignocellulosic biomass through proximate, ultimate and compositional analysis for bioenergy production,” *Renew. Energ.* 103, 490-500. DOI:10.1016/j.renene.2016.11.039
- Solihat, N.N., Fajriutami, T., Adi, D.T.N., Fatriasari, W., and Hermiati, E. (2017). “Reducing sugar production of sweet sorghum bagasse kraft pulp,” *AIP Conference Proceedings*. 1803, 20012. DOI: 10.1063/1.4973139
- Song, Y., Jiang, W., Zhang, Y., Wang, H., Zou, F., Yu, K., and Han, G. (2018). “A novel process of nanocellulose extraction from kenaf bast,” *Mater. Res. Express*. 5, 085032. DOI 10.1088/2053-1591/aac80d
- Tan, J. Y., Low, S. Y., Ban, Z. H., and Siwayanan, P. (2021). “A review on oil spill clean-up using bio-sorbent materials with special emphasis on utilization of kenaf core fibers,” *BioResources* 16(4), 8394-8416. DOI: 10.15376/biores.16.4.Tan
- Tang, Y., Shen, X., Zhang, J., Guo, D., Kong, F., and Zhang, N. (2015). “Extraction of cellulose nano-crystals from old corrugated container fiber using phosphoric acid and enzymatic hydrolysis followed by sonication,” *Carbohydr. Polym.* 125, 360-366. DOI: 10.1016/j.carbpol.2015.02.063
- Trilokesh, C., and Uppuluri, K. B. (2019). “Isolation and characterization of cellulose nanocrystals from jackfruit peel,” *Sci. Rep.* 9, 16709-16709. DOI: 10.1038/s41598-019-53412-x
- Wang, Z., Yao, Z., Zhou, J., and Zhang, Y. (2017). “Reuse of waste cotton cloth for the extraction of cellulose nanocrystals,” *Carbohydr. Polym.* 157, 945-952. DOI: 10.1016/j.carbpol.2016.10.044.
- Wang, Q., Xiao, S., Shi, S.Q., and Cai, L. (2018). “Effect of light-delignification on mechanical, hydrophobic, and thermal properties of high-strength molded fiber materials,” *Sci. Rep.* 8, 955. DOI: 10.1038/s41598-018-19623-4
- Webber, C. L. III. (1993). “Yield components of five kenaf cultivars,” *Agron. J.* 85(3), 533-535. DOI: 10.2134/agronj1993.00021196200850030002x
- Zaini, L. H., Jonoobi, M., Tahir, P. Md., and Karimi, S. (2013). “Isolation and characterization of cellulose whiskers from kenaf (*Hibiscus cannabinus* L.) bast fibers,” *J. Biomater. Nanobiotechnol.* 4, 37-44. DOI: 10.4236/jbnb.2013.41006
- Zarina, S., and Ahmad, I. (2015). “Biodegradable composite films based on κ -

carrageenan reinforced by cellulose nanocrystal from kenaf fibers,” *Bioresources* 10(1), 256-271. DOI: 10.15376/biores.10.1.256-271

Zhao, G., Kuang, G., Wang, Y., Yao, Y., Zhang, J., and Pan, Z.H. (2020). “Effect of steam explosion on physicochemical properties and fermentation characteristics of sorghum (*Sorghum bicolor* (L.) Moench),” *Lwt-Food Sci. Technol.* 129, 109579-109579. DOI: 10.1016/j.lwt.2020.109579

Zhang, Y., Haque, A. N. M. A., and Naebe, M. (2021). “Lignin-cellulose nanocrystals from hemp hurd as light-coloured ultraviolet (UV) functional filler for enhanced performance of polyvinyl alcohol nanocomposite films,” *Nanomater.* 11, 3425. DOI: 10.3390/nano11123425

Zhang, L., Larsson, A., Moldin, A., and Edlund, U. (2022). “Comparison of lignin distribution, structure, and morphology in wheat straw and wood,” *Ind. Crops Prod.* 187, 115432. DOI: 10.1016/j.indcrop.2022.115432

Article submitted: July 12, 2023; Peer review completed: July 29, 2023; Revised version received and accepted: August 3, 2023; Published: August 8, 2023.

DOI: 10.15376/biores.18.4.6913-6928